Achieving Full Frequency and Space Diversity in Wireless Systems via BICM, OFDM, STBC, and Viterbi Decoding

Enis Akay, *Student Member, IEEE*, and Ender Ayanoglu, *Fellow, IEEE*

***Abstract*—Orthogonal frequency-division multiplexing (OFDM) is known as an efficient technique to combat frequency-selective channels. In this paper, we show that the combination of bit-interleaved coded modulation (BICM) and OFDM achieves the full frequency diversity offered by a frequency-selective channel with any kind of power delay profile (PDP), conditioned on the minimum Hamming distance d_{free} of the convolutional code. This system has a simple Viterbi decoder with a modified metric. We then show that by combining such a system with space–time block coding (STBC), one can achieve the full space and frequency diversity of a frequency-selective channel with N transmit and M receive antennas. BICM-STBC-OFDM achieves the maximum diversity order of NML over L-tap frequency-selective channels regardless of the PDP of the channel. This latter system also has a simple Viterbi decoder with a properly modified metric. We verify our analytical results via simulations, including channels employed in the IEEE 802.11 standards.**

***Index Terms*—Bit-interleaved coded modulation (BICM), diversity, orthogonal frequency-division multiplexing (OFDM), space–time block coding (STBC), space–time frequency coding.**

I. Introduction

WIRELESS communication channels suffer from severe attenuation due to the destructive addition of multiple paths in the propagation media and from interference generated by other users. In some cases, it is impossible for the receiver to make a correct decision on the transmitted signal unless some form of diversity is employed. In order to combat severe conditions of wireless channels, different diversity techniques (such as temporal, frequency, spatial, and code diversity) have been developed.

Zehavi showed that code diversity could be improved by bitwise interleaving [1]. Following Zehavi's work, Caire *et al.* [2] presented the theory behind bit-interleaved coded modulation (BICM). Their work provided tools to evaluate the performance of BICM with tight error-probability bounds, and design guidelines.

In recent years, deploying multiple transmit antennas has become an important tool to improve diversity. The use of multiple transmit antennas allowed significant diversity gains for wireless communications. Space–time (ST) codes are an important class of spatial diversity systems, and some important results can be listed, as in [3]–[6]. In these papers, the multi-input multi-output (MIMO) wireless channel is assumed to be flat-fading. However, when there is frequency selectivity in the channel, the design of appropriate ST codes becomes a more complicated problem due to the existence of intersymbol interference (ISI). On the other hand, frequency-selective channels offer additional frequency diversity [7], [8], and carefully designed systems can exploit this property. Orthogonal frequency-division multiplexing (OFDM) is known to combat ISI very effectively, and therefore, can simplify the code-design problem for frequency-selective channels. Some ST-frequency-coded systems have been proposed to exploit the diversity order in space and frequency [9]–[17]. Out of these references, [15] combines space–time block codes (STBC) of [4] and [5] with BICM-OFDM to achieve diversity in space and frequency as illustrated via simulations. References [13], [14], and [16] use BICM-OFDM directly with multiple antennas and without external STBC to achieve a higher data rate at the cost of lower diversity.

In this paper, we separated the design of full space and frequency diversity codes into two. First, single-input single-output (SISO) wireless systems are considered. The significant advantages of BICM-OFDM of Section III over frequency-selective channels are presented. It is *formally proven* in Section IV that BICM-OFDM systems can achieve a diversity order of $\min(d_{\text{free}}, L)$ independent of the power delay profile (PDP) of the channel, where d_{free} is the minimum Hamming distance of the convolutional code, and L is the number of taps in the channel. As a result, we first show that BICM-OFDM systems provide codes that achieve full frequency diversity by using an appropriate convolutional code. Initial results on this subject, without the arbitrary PDP analysis developed in this paper, were presented in [18].

On the other hand, STBC makes use of diversity in the space domain by coding in space and time. Thus, by combining STBC with BICM-OFDM, as presented in Section V, we are able to add the spatial dimension to exploit diversity, as well. In Section VI, using the results of Section IV, we formally prove that BICM-STBC-OFDM systems achieve the diversity order of $NM\min(d_{\text{free}}, L)$, for systems employing N transmit and M receive antennas, over L-tap frequency-selective channels regardless of the PDP of the channel. In addition to analysis, through simulations, the performance of BICM-STBC-OFDM

Paper approved by Y. Li, the Editor for Wireless Communications Theory of the IEEE Communications Society. Manuscript received April 27, 2005; revised March 21, 2006. This paper was presented in part at the IEEE Vehicular Technology Conference, Los Angeles, CA, September 2004.

The authors are with the Center for Pervasive Communications and Computing, Department of Electrical Engineering and Computer Science, the Henry Samueli School of Engineering, University of California Irvine (e-mail: eakay@uci.edu; ayanoglu@uci.edu).

Digital Object Identifier 10.1109/TCOMM.2006.885089

as compared with [3] and [19] with OFDM is illustrated. Initial results on the diversity order of BICM-STBC-OFDM were presented in [17].

In the following sections, we provide step-by-step, clear proofs on the diversity order of BICM-OFDM and BICM-STBC-OFDM systems. In the Appendix, we show that the matrix $\mathbf{A}$, which is crucial to the pairwise error probability (PEP) analysis, can be decomposed into a multiplication of two Vandermonde matrices. Using the determinant property of Vandermonde matrices, we provide the rank of the matrix $\mathbf{A}$. In Section IV, the rank of $\mathbf{A}$ is shown to be the diversity order of the overall system by calculating the PEP. The decomposition presented in the Appendix is unique to this paper.

Unlike [13]–[16], our analysis does not require random ideal bit interleaving. In fact, by starting our PEP analysis between two binary codewords, we provide a very simple interleaver design criterion. Since convolutional codes are trellis-based, d_{free} distinct bits between any two codewords appear on a finite number of consecutive trellis branches which spans, in total, d bits. The interleaver should be designed such that d consecutive coded bits are mapped onto different symbols and transmitted over different OFDM subcarriers. The interleaver depth of only one OFDM symbol is also shown to be sufficient. The first permutation of the interleaver used in the IEEE 802.11a standard ensures that adjacent coded bits are mapped onto nonadjacent subcarriers [20], satisfying the design criterion presented here. When BICM-STBC-OFDM is implemented, we first place the K number of symbols (where K is the number of subcarriers in an OFDM symbol) in vectors and apply ST coding on these vectors. This way, the simple interleaver of BICM-OFDM can be used for BICM-STBC-OFDM as well.

Our analysis does not depend on the delay spread of the channel, whereas in [13] and [16], a large delay spread is assumed. We provide exact diversity orders for different delay spreads and for any convolutional code. In [13] and [14], the diversity order of the system is given to be dependent on the effective length of the space–frequency code. In this paper, we specifically show that the diversity order directly depends on the d_{free} of the convolutional code being used. Also, our MIMO system, BICM-STBC-OFDM, guarantees a higher diversity order. In other words, BICM-STBC-OFDM gives a diversity order of $NM\min(d_{\text{free}}, L)$ while the system in [13] and [14] provides diversity order of $M\min(F, NL)$ where F is the effective length of the space–frequency code. Higher diversity order of our MIMO system arises from the fact that we implement STBC, whereas in [13] and [14], there is no STBC. In order to achieve a high performance, [13] and [14] use iterative decoding. However, in this paper, we do not need, and therefore do not consider, iterative decoding for the reasons explained in the following sections. In [16], again assuming a large delay spread, the diversity order is given as Md_{free}.

Overall, in this paper, we provide two flexible systems, BICM-OFDM and BICM-STBC-OFDM, that can achieve the maximum diversity order available in the channel. Our proofs on the diversity orders of these systems do not require large delay spread and ideal interleaving assumptions. We present an easy-to-implement design criterion for the bit interleaver to achieve the maximum frequency diversity. We show that this simple interleaver can be used for our MIMO system, as well, as long as ST coding is applied on vectors of symbols. Unlike [12], the systems presented here do not require *a priori* knowledge of the delay spread of the channel to design the code. If that kind of knowledge is present and $d_{\text{free}} > L$, then puncturing can be used to increase the data rate while still achieving the maximum frequency diversity (given that d_{free} of the punctured code is at least L). Or, a higher rate, lower d_{free} (given $d_{\text{free}} \geq L$) best known convolutional code can be used to achieve the maximum diversity and a higher coding gain when compared with the punctured code.

We provide simulation results supporting our analysis in Section VII. Finally, the paper is concluded in Section VIII, where the important results of this paper are restated.

II. Bit-Interleaved Coded Modulation (BICM)

A BICM system can be obtained by using a bit interleaver π between an encoder for a binary code $\mathcal{C}$ and a memoryless modulator over a signal set $\chi \subseteq \mathbb{C}$ of size $|\chi| = M = 2^m$ with a binary labeling map $\mu : \{0,1\}^m \rightarrow \chi$. Gray labeling is used to map the bits onto symbols and plays an important role in the performance of BICM. It is shown in [21] that the capacity of BICM is surprisingly close to the capacity of a multilevel codes (MLC) scheme if and only if Gray labeling is used. Moreover, Gray labeling allows parallel independent decoding for each bit. In [21], it is actually recommended to use Gray labeling and BICM for fading channels. If set partition labeling or mixed labeling is used, then an iterative decoding approach can be used to achieve high performance [22]. Note that due to the ability of independent parallel decoding of Gray labeling, iterative decoding does not introduce any performance improvement [22]. Therefore, noniterative maximum-likelihood (ML) decoding (Viterbi algorithm) is considered in this paper.

During transmission, the code sequence $\underline{c}$ is interleaved by π, and then mapped onto the signal sequence $\underline{x} \in \chi$. The signal sequence $\underline{x}$ is then transmitted over the channel.

The bit interleaver can be modeled as $\pi : k' \rightarrow (k, i)$ where k' denotes the original ordering of the coded bits $c_{k'}$, k denotes the time ordering of the signals x_k transmitted, and i indicates the position of the bit $c_{k'}$ in the symbol x_k.

Let χ_b^i denote the subset of all signals $x \in \chi$ whose label has the value $b \in \{0,1\}$ in position i. Then, the ML bit metrics with the channel state information (CSI) can be given by

$$\lambda^i(y_k, c_{k'}) = \min_{x \in \chi_{c_{k'}}^i} \|y_k - \rho x\|^2 \tag{1}$$

where y_k is the received symbol at time k, ρ denotes the Rayleigh coefficient, and $\|(\cdot)\|^2$ represents the squared Euclidean norm of $(\cdot)$. Following (1), the ML decoder at the receiver can make decisions according to the rule

$$\hat{\underline{c}} = \arg\min_{\underline{c} \in \mathcal{C}} \sum_{k'} \lambda^i(y_k, c_{k'}). \tag{2}$$

III. BICM-OFDM

The system deploys only one transmit and one receive antenna (SISO). One OFDM symbol has K subcarriers, where each subcarrier corresponds to a symbol from a constellation

map χ. As given in Section II, constellation size $|\chi| = 2^m$. A convolutional encoder is used to generate the binary code at the transmitter. For the k_0/n_0-rate convolutional code with a given number of states, the one with the highest minimum Hamming distance d_{free} is picked from tables, e.g., [23]. The output bit $c_{k'}$ of a convolutional encoder is interleaved and mapped onto the subcarrier $x(k)$ at the ith location. The interleaver should be designed such that consecutive coded bits are:

1) mapped onto different symbols;
2) transmitted over different subcarriers;
3) interleaved within one OFDM symbol to avoid an extra delay requirement to start decoding at the receiver.

Consider a frequency-selective channel with L taps given by $\underline{\mathrm{h}} = [h_0\, h_1\, \ldots\, h_{(L-1)}]^T$. Each tap is assumed to be statistically independent and modeled as a zero-mean complex Gaussian random variable with unit variance. The fading model is assumed to be quasi-static, i.e., the fading coefficients are constant over the transmission of one packet, but independent from one packet transmission to the next. It is assumed that the taps are spaced at integer multiples of the symbol duration, which is the worst-case scenario in terms of designing full diversity codes [24].

A cyclic prefix (CP) of appropriate length is added to each OFDM symbol. Adding CP converts the linear convolution of the transmitted signal and the L-tap channel into a circular convolution. When CP is removed and fast Fourier transform (FFT) is taken at the receiver, the received signal is given by

$$y(k) = H(k)x(k) + n(k), \quad 0 \le k \le K-1 \tag{3}$$

where $x(k)$ is the transmitted signal at the kth subcarrier, $n(k)$ is complex additive white Gaussian noise (AWGN) with zero mean and variance $N_0 = 1/\text{SNR}$, and $H(k)$ is given by

$$H(k) = \underline{\mathrm{W}}_K^H(k)\mathbf{P}\underline{\mathrm{h}} \tag{4}$$

where $\underline{\mathrm{W}}_K(k) = [1\ W_K^k\ W_K^{2k}\ \ldots\ W_K^{(L-1)k}]^H$ is an $L \times 1$ vector with $W_K \triangleq e^{-j2\pi/K}$, and $\mathbf{P}$ is an $L \times L$ diagonal matrix with p_l, for $l = 0, \ldots, L-1$, on the main diagonal representing the PDP of the frequency-selective channel $\underline{\mathrm{h}}$. PDP matrix entries p_l's are real and strictly positive. Note that the transmitted symbols are assumed to have average energy of 1, and $\sum_{l=0}^{L-1} p_l^2 = 1$. Consequently, with the channel, PDP, and AWGN models described here, the received signal-to-noise ratio is SNR.

IV. Diversity Order of BICM-OFDM

In this section, the PEP analysis of the system described in Section III is provided. It will be shown that for an L-tap frequency-selective channel with any type of PDP, BICM-OFDM can achieve a diversity order of $\min(d_{\text{free}}, L)$ without the use of multiple antennas. Since d_{free} of convolutional codes can be large, this is a significant result.

Assume the code sequence $\underline{\mathrm{c}}$ is transmitted and $\underline{\hat{\mathrm{c}}}$ is detected. Then, the PEP of $\underline{\mathrm{c}}$ and $\underline{\hat{\mathrm{c}}}$ given CSI can be written as, using (1) and (2)

$$P(\underline{\mathrm{c}} \to \underline{\hat{\mathrm{c}}}|\mathbf{H}) = P\left(\sum_{k'} \min_{x \in \chi^i_{c_{k'}}} \|y(k) - H(k)x\|^2 \ge \sum_{k'} \min_{x \in \chi^i_{\hat{c}_{k'}}} \|y(k) - H(k)x\|^2\right). \tag{5}$$

Assume $d(\underline{\mathrm{c}} - \underline{\hat{\mathrm{c}}}) = d_{\text{free}}$ for $\underline{\mathrm{c}}$ and $\underline{\hat{\mathrm{c}}}$ under consideration for PEP analysis, which is the smallest Hamming distance between any two codewords. Then, $\chi^i_{c_{k'}}$ and $\chi^i_{\hat{c}_{k'}}$ are equal to one another for all k' except for d_{free} distinct values of k'. Therefore, the inequality on the right-hand side of (5) shares the same terms on all but d_{free} summation points, and the summations can be simplified to only d_{free} terms for PEP analysis. Note that for binary codes and for the d_{free} points at hand, $\hat{c}_{k'} = \bar{c}_{k'}$, where $\bar{(\cdot)}$ denotes the binary complement of $(\cdot)$. For the d_{free} bits, let us denote

$$\tilde{x}(k) = \arg \min_{x \in \chi^i_{c_{k'}}} |y(k) - H(k)x|^2$$
$$\hat{x}(k) = \arg \min_{x \in \chi^i_{\bar{c}_{k'}}} |y(k) - H(k)x|^2. \tag{6}$$

It is easy to see that $\tilde{x}(k) \ne \hat{x}(k)$ since $\tilde{x}(k) \in \chi^i_{c_{k'}}$ and $\hat{x}(k) \in \chi^i_{\bar{c}_{k'}}$, where $\chi^i_{c_{k'}}$ and $\chi^i_{\bar{c}_{k'}}$ are complementary sets of constellation points within the signal constellation set χ. Also, $\|y(k) - x(k)H(k)\|^2 \ge \|y(k) - \tilde{x}(k)H(k)\|^2$, and the transmitted signal $x(k) \in \chi^i_{c_{k'}}$.

For convolutional codes, d_{free} distinct bits between any two codewords occur on a finite number of consecutive trellis branches which span, in total, d bits. The bit interleaver should be designed such that d consecutive coded bits are mapped onto different symbols and transmitted over different subcarriers (design criteria 1 and 2). This guarantees that there exists d_{free} distinct pairs of $(\tilde{x}(k), \hat{x}(k))$, and d_{free} distinct pairs of $(x(k), \hat{x}(k))$. Note that if there is no bit interleaver following the encoder, the number of distinct pairs is significantly lower. The PEP can be rewritten as

$$P(\underline{\mathrm{c}} \to \underline{\hat{\mathrm{c}}}|\mathbf{H}) = P\left(\sum_{k, d_{\text{free}}} |y(k) - H(k)\tilde{x}(k)|^2 - |y(k) - H(k)\hat{x}(k)|^2 \ge 0\right) \le Q\left(\sqrt{\frac{\sum_{k, d_{\text{free}}} d_{\min}^2 \|H(k)\|^2}{2N_0}}\right) \tag{7}$$

where $\sum_{k, d_{\text{free}}}$ means that the summation is taken with index k over d_{free} different values of k, and $d_{\min}$ denotes the minimum

Euclidean distance between two symbols on the constellation. Using (4)

$$\begin{aligned}\sum_{k,d_{\text{free}}} |H(k)|^2 &= \sum_{k,d_{\text{free}}} \underline{\mathrm{h}}^H \mathbf{P} \underline{\mathbf{W}}_K(k) \underline{\mathbf{W}}_K^H(k) \mathbf{P} \underline{\mathrm{h}} \\ &= \underline{\mathrm{h}}^H \mathbf{P} \left[\sum_{k,d_{\text{free}}} \underline{\mathbf{W}}_K(k) \underline{\mathbf{W}}_K^H(k) \right] \mathbf{P} \underline{\mathrm{h}} \\ &= \underline{\mathrm{h}}^H \mathbf{P} \left[\sum_{k,d_{\text{free}}} \mathbf{A}_k \right] \mathbf{P} \underline{\mathrm{h}} \\ &= \underline{\mathrm{h}}^H \mathbf{P} \mathbf{A} \mathbf{P} \underline{\mathrm{h}} \\ &= \underline{\mathrm{h}}^H \mathbf{B} \underline{\mathrm{h}} \end{aligned} \tag{8}$$

where $\mathbf{A}$, $\mathbf{B}$, and $\mathbf{A}_k$'s are $L \times L$ matrices and $\mathbf{A}_k = \underline{\mathbf{W}}_K(k) \underline{\mathbf{W}}_K^H(k)$ with rank one. However, due to the special form of the $\mathbf{A}_k$ matrices, the rank of the matrix $\mathbf{A} = \sum_{k,d_{\text{free}}} \mathbf{A}_k$ is $r = \text{rank}(\mathbf{A}) = \min(d_{\text{free}}, L)$ (see the Appendix for the proof). Since $\mathbf{P}$ is a nonsingular matrix, $\mathbf{B} = \mathbf{PAP}$ has rank $r = \min(d_{\text{free}}, L)$. Note that $\mathbf{A}_k$s are positive semidefinite Hermitian, and so are $\mathbf{A}$ and $\mathbf{B}$ [3], [25]. Consequently, the singular value decomposition (SVD) of $\mathbf{B}$ can be written as [25]

$$\mathbf{B} = \mathbf{V} \mathbf{\Lambda} \mathbf{V}^H \tag{9}$$

where $\mathbf{V}$ is an $L \times L$ unitary matrix, and $\mathbf{\Lambda}$ is an $L \times L$ diagonal matrix with eigenvalues of $\mathbf{B}$, $\{\lambda_i(\mathbf{B})\}_{i=0}^{L-1}$ in decreasing order (which are real and nonnegative), on the main diagonal.

According to Ostrowski's theorem, for each $i = 0, 1, \ldots, L-1$, there exists a positive real number θ_i such that $\lambda_{L-1}(\mathbf{P}^2) \le \theta_i \le \lambda_0(\mathbf{P}^2)$ and $\lambda_i(\mathbf{B}) = \theta_i \lambda_i(\mathbf{A})$ [25]. Since $\mathbf{P}^2$ is a diagonal matrix, the minimum eigenvalue of $\mathbf{P}^2$, $\lambda_{L-1}(\mathbf{P}^2) = \lambda_{\min}(\mathbf{P}^2) = \min_i p_i^2 \triangleq p_{\min}^2$. Consequently, $\lambda_i(\mathbf{B}) \ge p_{\min}^2 \lambda_i(\mathbf{A})$ for $i = 0, 1, \ldots, L-1$.

Let us denote the elements of the vector $\mathbf{V}^H \underline{\mathrm{h}}$ as v_i for $i = 0, 1, \ldots, L-1$. Note that $|v_i|$s are Rayleigh distributed with probability density function (pdf) $2|v_i| e^{-|v_i|^2}$. Using an upper bound for the Q function $Q(x) \le (1/2) e^{-x^2/2}$, PEP can be written as

$$\begin{aligned} P(\underline{\mathrm{c}} \to \hat{\underline{\mathrm{c}}}) &= E\left[P(\underline{\mathrm{c}} \to \hat{\underline{\mathrm{c}}} | \mathbf{H}) \right] \\ &\le E\left[\frac{1}{2} \exp\left(- \frac{d_{\min}^2 p_{\min}^2 \sum_{i=0}^{L-1} \lambda_i(\mathbf{A}) |v_i|^2}{4N_0} \right) \right] \\ &= \frac{1}{2} \prod_{i=0}^{L-1} \left(1 + \frac{d_{\min}^2 p_{\min}^2 \lambda_i(\mathbf{A})}{4N_0} \right)^{-1} \\ &\simeq \left(\prod_{i=0}^{r-1} \lambda_i(\mathbf{A}) \right)^{-1} \left(\frac{d_{\min}^2 p_{\min}^2 \text{SNR}}{4} \right)^{-r} \end{aligned} \tag{10}$$

for high SNR. It can be easily seen from (10) that the diversity order of BICM-OFDM system is $r = \min(d_{\text{free}}, L)$ regardless of the PDP of the frequency-selective channel. Note that the smallest upper bound is given for equal PDP, where $p_0^2 = p_1^2 = \ldots = p_{L-1}^2 = p_{\min}^2 = 1/L$. The industry standard 1/2-rate 64-state (133,171) convolutional encoder has $d_{\text{free}} = 10$. Therefore, a BICM-OFDM system with this convolution code can achieve a diversity order of 10 without implementing any additional antennas, or using any other diversity technique. In order to even further increase the diversity order of the system, one can, in addition, add multiple antennas using STBC to multiply the diversity order of BICM-OFDM with the number of transmit and receive antennas (see Section VI). Or, multiple antennas can be used to increase the throughput of the system, while BICM-OFDM is used to provide the necessary diversity order. Also, a low-complexity Viterbi decoder can be implemented for BICM-OFDM systems without any performance degradation [26], [27]. Thus, a low-complexity, easy-to-implement, and a high-diversity-order system can be easily generated by BICM-OFDM.

V. BICM-STBC-OFDM

In this section, we consider complex orthogonal STBCs [5]. For N transmit antennas, S/T-rate STBC is defined as the complex orthogonal block code which transmits S symbols over T time slots. The code generator matrix $\mathbf{G}_{STN}$ is a $T \times N$ matrix and satisfies [5]

$$\mathbf{G}_{STN}^H \mathbf{G}_{STN} = \kappa \left(|x_1|^2 + |x_2|^2 + \ldots + |x_S|^2 \right) \mathbf{I}_N \tag{11}$$

where κ is a positive constant, $\{x_i\}_{i=1}^S$ are the complex symbols transmitted in one STBC codeword, and $\mathbf{I}_N$ is the $N \times N$ identity matrix. For example, Alamouti code [4] is a rate-one STBC given as

$$\mathbf{G}_{222} = \begin{bmatrix} x_1 & x_2 \\ -x_2^* & x_1^* \end{bmatrix}. \tag{12}$$

In BICM-STBC-OFDM, a rate-S/T STBC is used to code the tones of an OFDM symbol across time and space, and BICM is applied for coded modulation. After interleaving, the output bit $c_{k'}$ is mapped onto the tone $x_s(k)$ at the ith bit location, where $1 \le s \le S$. As shown in Fig. 1, once the coded bits are mapped onto symbols, K consecutive symbols are converted from serial to parallel. ST coding is then applied on the vectors of symbols of length K. By doing so, the simple interleaver of BICM-OFDM can be used, such that adjacent coded bits are mapped onto different subcarriers. It is assumed that an appropriate length of CP is used for each OFDM symbol. As a result, the received signal for each tone is given by the $T \times M$ matrix

$$\mathbf{R}(k) = \mathbf{C}(k) \mathbf{H}(k) + \mathbf{N}(k) \tag{13}$$

where $\mathbf{C}(k) = \mathbf{G}_{STN}(x_1(k), \ldots, x_S(k))$, which is calculated by applying the symbols $x_1(k), \ldots, x_S(k)$ to the STBC generator matrix $\mathbf{G}_{STN}$, and $\mathbf{N}(k)$ is a $T \times M$ complex AWGN with

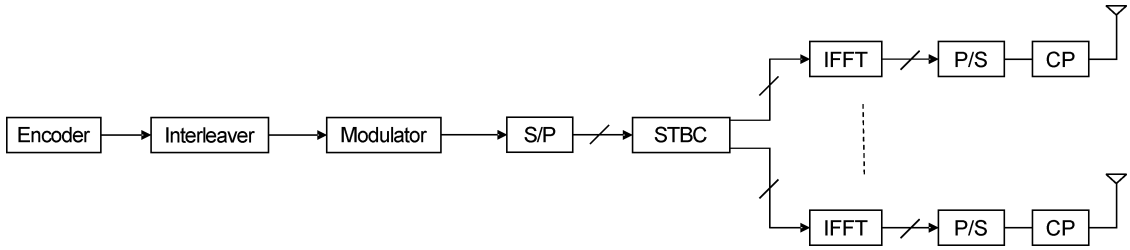

Fig. 1. Block diagram of BICM-STBC-OFDM.

zero mean and variance $N_0 = N/\text{SNR}$. $N \times M$ channel matrix $\mathbf{H}(k)$, at the kth subcarrier, is given by

$$\begin{aligned}\mathbf{H}(k) &= \mathbf{W}_K^H(k)\mathbf{P}_F\mathbf{h}\\ \mathbf{W}_K(k) &= \mathbf{I}_N \otimes \underline{\mathrm{W}}_K(k),\\ \mathbf{P}_F &= \mathbf{I}_N \otimes \mathbf{P}\\ \mathbf{h} &= \begin{bmatrix} \underline{\mathrm{h}}_{11} & \underline{\mathrm{h}}_{12} & \cdots & \underline{\mathrm{h}}_{1M} \\ \underline{\mathrm{h}}_{21} & \underline{\mathrm{h}}_{22} & \cdots & \underline{\mathrm{h}}_{2M} \\ \vdots & \vdots & \ddots & \vdots \\ \underline{\mathrm{h}}_{N1} & \underline{\mathrm{h}}_{N2} & \cdots & \underline{\mathrm{h}}_{NM} \end{bmatrix}_{NL\times M}\end{aligned} \tag{14}$$

where $\otimes$ denotes the Kronecker product of two matrices, $\underline{\mathrm{W}}_K(k)$ and $\mathbf{P}$ are as defined in Section III, and $\underline{\mathrm{h}}_{nm}$ is the $L\times 1$ vector representing the L-tap frequency-selective channel from the transmit antenna n to the receive antenna m. Each tap is assumed to be statistically independent and modeled as a zero-mean complex Gaussian random variable with unit variance. The fading model is assumed to be quasi-static. Note that the average energy transmitted from each antenna at each subcarrier is assumed to be 1. Then, with the given channel, PDP, and noise models, the received SNR is SNR. Also note that from now on, we deviate from the notation of (3) as to the order of $\mathbf{C}(k)$ and $\mathbf{H}(k)$ because of the convention in the literature for STBC [28].

VI. Diversity Order of BICM-STBC-OFDM

In this section, by calculating the PEP, it will be shown that BICM-STBC-OFDM can achieve the maximum achievable diversity order of NML. Assume that binary codeword $\underline{\mathrm{c}}$ is sent and $\hat{\underline{\mathrm{c}}}$ is detected. Then, the PEP, given channel information, is written as

$$\begin{aligned}P(\underline{\mathrm{c}} \to \hat{\underline{\mathrm{c}}}|\mathbf{H}) &= P\left(\sum_{k'} \min_{x_s \in \chi^i_{c_{k'}}} \|\mathbf{R}(k) - \mathbf{C}\mathbf{H}(k)\|_F^2 \right.\\ &\qquad \left. \geq \sum_{k'} \min_{x_s \in \chi^i_{\hat{c}_{k'}}} \left\|\mathbf{R}(k) - \hat{\mathbf{C}}\mathbf{H}(k)\right\|_F^2\right)\end{aligned} \tag{15}$$

where $\|(\cdot)\|_F^2$ denotes $\|(\cdot)\|_F^2 = Tr\{(\cdot)^H(\cdot)\}$ [square of the Frobenius norm of $(\cdot)$], and $\mathbf{C}$ and $\hat{\mathbf{C}}$ denote the two distinct STBC codewords.

Note that $\|\mathbf{R}(k) - \mathbf{C}\mathbf{H}(k)\|_F^2$ provides S equations to decode S symbols within STBC $\mathbf{C}$ [5], [6]. As mentioned in Section V, the output bit $c_{k'}$ is mapped onto the ith bit of $x_s(k)$. So the bit metric for each $c_{k'}$ is found by minimizing the sth equation given by $\|\mathbf{R}(k) - \mathbf{C}\mathbf{H}(k)\|_F^2$ with respect to $x_s \in \chi^i_{c_{k'}}$.

Similar to Section IV, by defining

$$\begin{aligned}\tilde{\mathbf{C}}(k) &= \arg \min_{\substack{\mathbf{C}=\mathbf{G}_{STN}(x_1,\ldots,x_S)\\ \text{s.t. } x_s \in \chi^i_{c_{k'}}}} \|\mathbf{R}(k) - \mathbf{C}\mathbf{H}(k)\|_F^2\\ \hat{\mathbf{C}}(k) &= \arg \min_{\substack{\hat{\mathbf{C}}=\mathbf{G}_{STN}(x_1,\ldots,x_S)\\ \text{s.t. } x_s \in \chi^i_{\hat{c}_{k'}}}} \|\mathbf{R}(k) - \mathbf{C}\mathbf{H}(k)\|_F^2\end{aligned} \tag{16}$$

where $\tilde{\mathbf{C}}(k)$ and $\hat{\mathbf{C}}(k)$ are distinct two STBC matrices, and $\mathbf{C}(k)$ is the transmitted STBC, (15) can be rewritten as

$$\begin{aligned}P(\underline{\mathrm{c}} \to \hat{\underline{\mathrm{c}}}|\mathbf{H}) &\leq P\left(\beta \geq \sum_{k,d_{\text{free}}} \left\|\left(\mathbf{C}(k) - \hat{\mathbf{C}}(k)\right)\mathbf{H}(k)\right\|_F^2\right)\\ &= Q\left(\sqrt{\frac{\sum_{k,d_{\text{free}}} \left\|\left(\mathbf{C}(k) - \hat{\mathbf{C}}(k)\right)\mathbf{H}(k)\right\|_F^2}{2N_0}}\right)\end{aligned} \tag{17}$$

where $\beta = \sum_{k,d_{\text{free}}} \beta(k)$, and $\beta(k) = Tr\{\mathbf{H}^H(k)(\hat{\mathbf{C}}(k) - \mathbf{C}(k))^H\mathbf{N}(k) + \mathbf{N}^H(k)(\hat{\mathbf{C}}(k) - \mathbf{C}(k))\mathbf{H}\}$. Consequently, β is a zero-mean Gaussian random variable with variance $2N_0 \sum_{k,d_{\text{free}}} \|(\hat{\mathbf{C}}(k) - \mathbf{C}(k))\mathbf{H}\|_F^2$.

Let us define $\mathbf{D}(k) = \mathbf{C}(k) - \hat{\mathbf{C}}(k)$, which is still a $T \times N$ complex orthogonal design. $\mathbf{D}^H(k)\mathbf{D}(k) = |d(k)|^2\mathbf{I}_N$, where $|d(k)|^2 = \kappa(|d_1(k)|^2 + |d_2(k)|^2 + \ldots + |d_S(k)|^2)$ is a positive constant with $d_i(k)$'s denoting the S complex numbers of $\mathbf{D}(k)$. $\mathbf{C}(k)$ and $\hat{\mathbf{C}}(k)$ differ in at least at one symbol. Therefore, $|d(k)|^2 \geq \kappa d_{\min}^2$. It follows that

$$\begin{aligned}\sum_{k,d_{\text{free}}} \|\mathbf{D}(k)\mathbf{H}(k)\|_F^2 &= \sum_{k,d_{\text{free}}} |d(k)|^2 Tr\left\{\mathbf{H}^H(k)\mathbf{H}(k)\right\}\\ &\geq \kappa d_{\min}^2 Tr\left\{\mathbf{h}^H\mathbf{P}_F(\mathbf{I}_N \otimes \mathbf{A})\mathbf{P}_F\mathbf{h}\right\}\\ &= Tr\{\mathbf{h}^H\mathbf{Z}\mathbf{h}\}\end{aligned} \tag{18}$$

where

$$\begin{aligned}\mathbf{Z} &= \mathbf{I}_N \otimes \mathbf{B}\\ \mathbf{B} &= \mathbf{P}\mathbf{A}\mathbf{P}\\ \mathbf{A} &= \sum_{k,d_{\text{free}}} \mathbf{A}_k\\ \mathbf{A}_k &= \underline{\mathrm{W}}_K(k)\underline{\mathrm{W}}_K^H(k).\end{aligned} \tag{19}$$

Note that the $NL \times NL$ matrix $\mathbf{Z}$ is positive semidefinite, and has rank $N\min(d_{\text{free}}, L)$, and, as shown in Section IV, $\mathbf{A}$

has rank $r = \min(d_{\text{free}}, L)$. The SVD and the eigenvalues of $\mathbf{Z}$ can be given as (recalling Ostrowski's theorem)

$$\begin{aligned} \mathbf{Z} &= \mathbf{V}_Z \mathbf{\Lambda}_Z \mathbf{V}_Z^H \\ \lambda_i(\mathbf{Z}) &= \lambda_{\lfloor i/N \rfloor}(\mathbf{B}) \geq p_{\min}^2 \lambda_{\lfloor i/N \rfloor}(\mathbf{A}), \quad i = 0, \ldots, NL-1 \end{aligned} \tag{20}$$

where $\lfloor(\cdot)\rfloor$ is the floor function, and the eigenvalues are in decreasing order with index i.

Let us denote the elements of $\mathbf{V}_Z^H \mathbf{h}$ with v_{ij}, for $i = 0, 1, \ldots, NL-1$ and $j = 0, 1, \ldots, M-1$. Note that $|v_{ij}|$'s are Rayleigh distributed with $2|v_{ij}|e^{-|v_{ij}|^2}$. Similar to Section IV

$$\begin{aligned} &P(\underline{c} \to \hat{\underline{c}}) \\ &\leq E\left[\frac{1}{2}\exp\left(-\frac{\kappa d_{\min}^2 p_{\min}^2 \sum_{j=0}^{M-1}\sum_{i=0}^{NL-1} \lambda_{\lfloor i/N \rfloor}(\mathbf{A})|v_{ij}|^2}{4N_0}\right)\right] \\ &= \frac{1}{2}\prod_{i=0}^{r-1}\left(1 + \frac{\kappa d_{\min}^2 p_{\min}^2 \lambda_i(\mathbf{A})\text{SNR}}{4N}\right)^{-NM} \\ &\simeq \frac{1}{2}\left(\prod_{i=0}^{r-1}\lambda_i(\mathbf{A})\right)^{-NM}\left(\frac{\kappa d_{\min}^2 p_{\min}^2 \text{SNR}}{4N}\right)^{-NMr} \end{aligned} \tag{21}$$

for high SNR. It is clearly evident from (21) that the BICM-STBC-OFDM system successfully achieves the diversity order of $NM\min(d_{\text{free}}, L)$. Note that, unlike [12], *a priori* knowledge of the delay spread is not necessary to design specific codes. If that kind of knowledge exists, puncturing can be used to increase the data rate while achieving the maximum frequency diversity for low-delay-spread channels. Or, a higher rate, lower d_{free} best known convolutional code can used to achieve the maximum frequency diversity, while having a higher coding gain compared with the punctured code. Indoor channels are, in general, highly frequency-selective for a typical office environment. Consequently, the proposed system achieves a higher diversity order than the one presented in [13] and [14], when the industry standard 64-state $d_{\text{free}} = 10$ convolutional code is used.

A low-complexity decoder for BICM-STBC-OFDM can be implemented using [29]. Hence, BICM-STBC-OFDM provides a low-complexity, easy-to-implement system with a high diversity order.

VII. Simulation Results

In the simulations of this section, 64 subcarriers are used for each OFDM symbol. One symbol has a duration of 4 μs, of which 0.8 μs is CP. 1000 bytes of information bits are sent with each packet, and the channel is assumed to be the same through the transmission of one packet. Coded bits are interleaved with the interleaver given in [20], and modulated onto symbols using 16-QAM with Gray labeling.

A. Diversity Order of BICM-OFDM

Figs. 2 and 3 show the simulation results for different root mean square (rms) delay-spread values of the frequency-selective channel with equal power taps with 64-state and 4-state convolutional encoders, respectively. As can be seen from Fig. 2, as the number of taps of the channel increases, the diversity order of BICM-OFDM increases as well to the maximum value of 10. Another interesting observation is that while diversity order for 50 ns and 75 ns channels reach the maximum value, the 75 ns channel shows a slightly better coding gain.

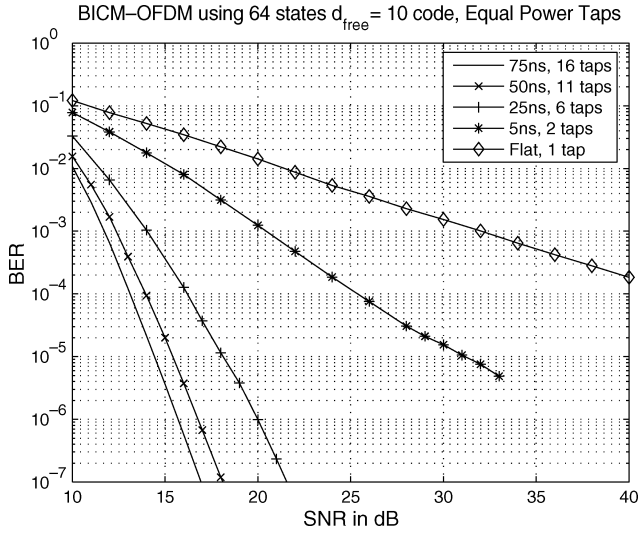

Fig. 2. BICM-OFDM results using 1/2–rate 64-state $d_{\text{free}} = 10$ convolutional encoder.

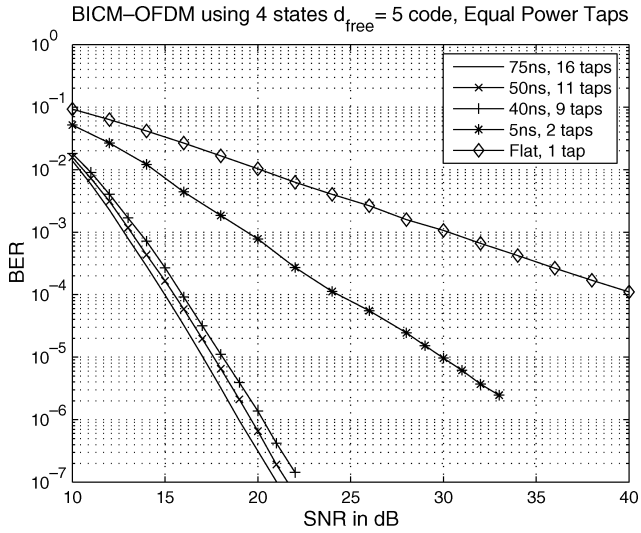

Fig. 3. BICM-OFDM results using 1/2-rate 4-state $d_{\text{free}} = 5$ convolutional encoder.

From Fig. 3, it is clearly evident that as the number of taps for the channel increases, the diversity order increases, as well. It can be seen that the maximum diversity order that can be achieved by $d_{\text{free}} = 5$ BICM-OFDM is 5. Similar to the results shown in Fig. 2, while diversity for 40, 50, and 75 ns channels reach the maximum value (i.e., all the curves have the same slope for high SNR values), the 75 ns channel shows a slightly better coding gain.

Fig. 4 illustrates the results of BICM-OFDM over equal power taps, and taps with exponential PDP. As can be seen, BICM-OFDM achieves full frequency diversity for different kinds of PDP at asymptotically high SNR values.

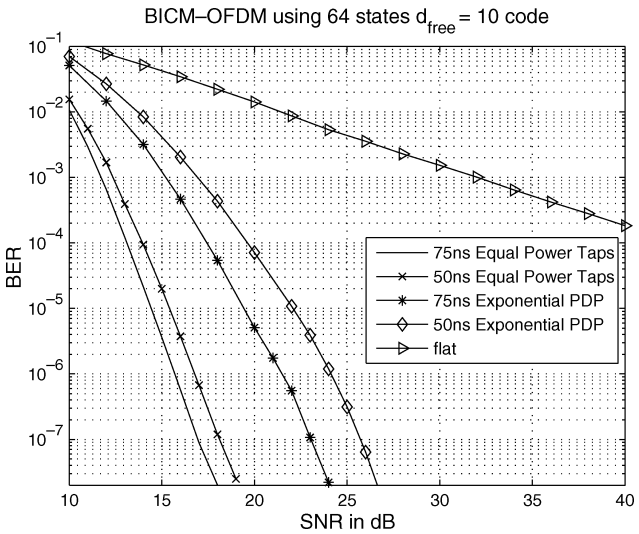

Fig. 4. BICM-OFDM results using 1/2-rate 64-state $d_{\text{free}} = 10$ code over equal power taps, and taps with exponential PDP.

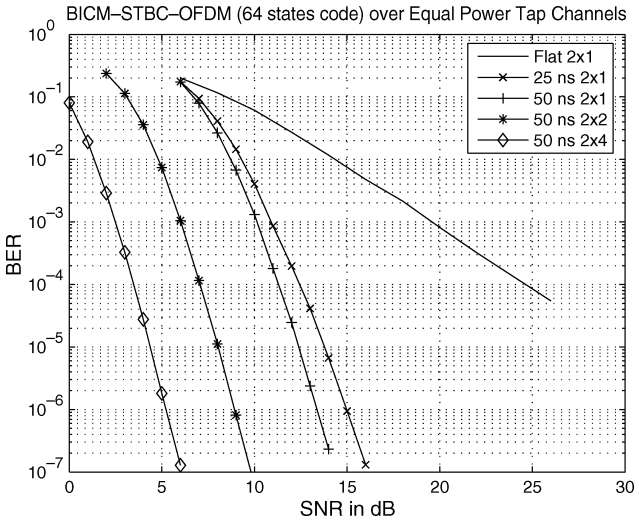

Fig. 5. BICM-STBC-OFDM results using 1/2-rate 64-state $d_{\text{free}} = 10$ code.

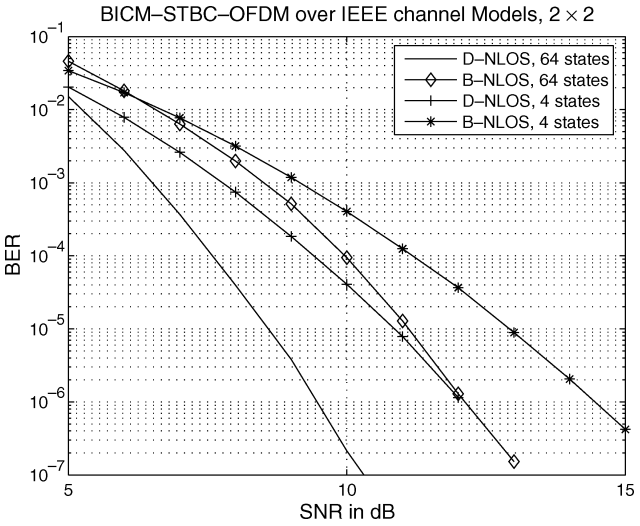

Fig. 6. BICM-STBC-OFDM results using 1/2-rate 64-state $d_{\text{free}} = 10$ code over IEEE channels.

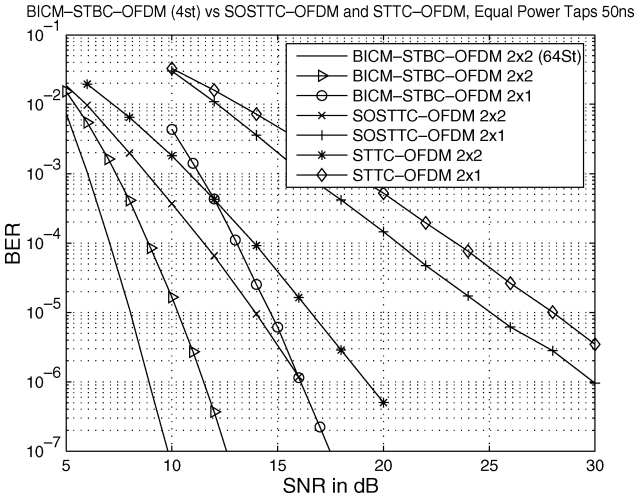

Fig. 7. Comparison between BICM-STBC-OFDM, SOSTTC-OFDM, and STTC-OFDM over equal power taps frequency-selective channel with 50 ns rms delay spread.

B. Diversity Order of BICM-STBC-OFDM

The system has two transmit antennas, and Alamouti's code [4] is used to implement BICM-STBC-OFDM.

Fig. 5 shows the results for the 1/2-rate 64-state $d_{\text{free}} = 10$ convolutional code. It can be seen from the figures that as the number of taps increases in the channel, the diversity order of BICM-STBC-OFDM increases up to the maximum diversity of $NM \min(d_{\text{free}}, L)$. Note that as the number of receive antennas is increased, the diversity order gets multiplied in the figures. For the two-transmit four-receive antenna case, even at low SNR values, the performance curve is extremely steep.

The simulation results for IEEE channel models [30]–[32] are given in Fig. 6. The channel models B and D have 9 and 18 taps, respectively, with the PDPs given in [30]. The indoor channel models are highly frequency-selective, and hence, our proposed MIMO system achieves a high diversity order.

Figs. 7 and 8 show the performance curves for 4-state BICM-STBC-OFDM, 4-state quaternary phase-shift keying (QPSK) super-orthogonal space–time trellis code (SOSTTC) [19] with OFDM, and 4-state QPSK space–time trellis code (STTC) [3] with OFDM. 4-state 1/2-rate $d_{\text{free}} = 5$ convolutional code [23] with 16-QAM modulation is used for BICM-STBC-OFDM, so that all the systems transmit 2 bits at each subcarrier. The channel is modeled as an equal power taps frequency-selective channel with 50 ns rms delay spread in Fig. 7. For the 2×1 case, 4-state BICM-STBC-OFDM outperforms SOSTTC-OFDM and STTC-OFDM by more than 10 and 13 dB, respectively. For the 2×2 case, the performance gain is more than 3.5 and 6.5 dB. If a 64-state convolutional code is used, then the performance gain is increased to 5.5 and 8.5 dB. Fig. 8 illustrates the results for IEEE Channel Models B and D. As can be seen, the performance gain is significant. This is mainly due the fact that SOSTTC and STTC were not designed to fully exploit the frequency diversity that is available in the channel. What we want to illustrate is that it is crucial and very beneficial to exploit, if it exists, the frequency selectivity of the channel. Also, by using the decoding scheme given in

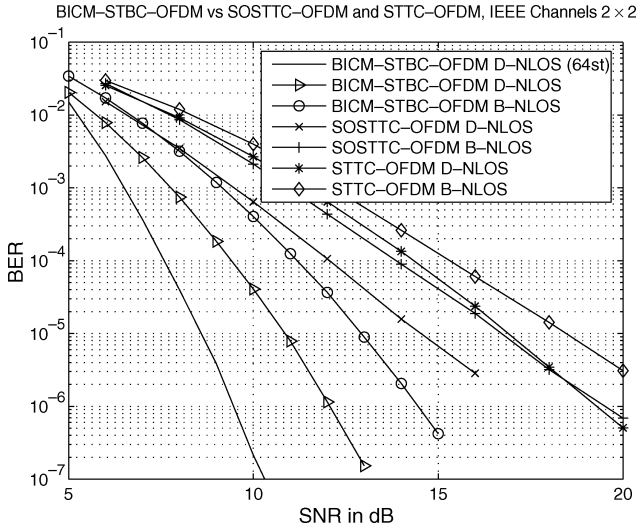

Fig. 8. Comparison between BICM-STBC-OFDM, SOSTTC-OFDM, and STTC-OFDM over IEEE Channel Models B and D.

[29], one can show that BICM-STBC-OFDM has a very low decoding complexity.

VIII. Conclusion

BICM and OFDM are used widely in many wireless communication systems. In this paper, it is shown that the two can be combined to achieve a high diversity order. It is illustrated both analytically and via simulations that the maximum diversity that is inherited in frequency-selective channels can be fully and successfully achieved. If a convolutional code is used with a minimum Hamming distance of d_{free}, it is shown that the diversity order of BICM-OFDM is $\min(d_{\text{free}}, L)$ for an L-tap frequency-selective fading channel with any kind of PDP. Simulations also showed that when $L \geq d_{\text{free}}$, as the delay spread increases, the coding gain increases, improving the system performance.

The BICM-STBC-OFDM system is introduced in order to exploit diversity in space as well as in frequency. It is shown both analytically and via simulations that BICM-STBC-OFDM reaches the maximum diversity order that can be offered by the channel. If the convolutional code being used has a minimum Hamming distance of d_{free}, it is shown that the diversity order of BICM-STBC-OFDM is $NM \min(d_{\text{free}}, L)$ for a system with N transmit and M receive antennas over an L-tap frequency-selective fading channel, regardless of the PDP of the channel.

Easy to implement interleaver design criteria to achieve the maximum frequency diversity is presented. Complete, clear, and unique proofs of diversity orders of BICM-OFDM and BICM-STBC-OFDM systems for any delay spread and for any convolutional code are given.

There exist low-complexity implementations of both systems presented. Hence, the two proposed schemes offer high performance (high diversity order), low complexity, and easy-to-implement systems.

Appendix
Proof of Rank $\min(d_{\text{free}}, L)$

Note that, in general, the number of subcarriers $K \geq d_{\text{free}}$ and $K \geq L$, and these are assumed to be the case in this paper. In order to have a clearer presentation, let us denote $D = d_{\text{free}}$ and without loss of generality, the D different $\mathbf{A}_k$ matrices can be reordered (or redefined) such that $\mathbf{A} = \sum_{k=1}^{D} \mathbf{A}_k$. Assume for now that $D \leq L$. Then, it is known that [25] rank $(\mathbf{A}) = r \leq \sum_{k=1}^{D} \text{rank}(\mathbf{A}_k) = D$. Let us denote $a_k \stackrel{\triangle}{=} W_K^k$. Note that $a_k^{-1} = a_k^*$, and a_k's lie on the unit circle on the complex plane and $a_i \neq a_j$ for $i \neq j$, $1 \leq i, j \leq K$. Then $\mathbf{A}_k$'s can be rewritten as

$$\mathbf{A}_k = \begin{bmatrix} 1 & a_k & \cdots & a_k^{(L-1)} \\ a_k^{-1} & 1 & \cdots & a_k^{(L-2)} \\ \vdots & \vdots & \ddots & \vdots \\ a_k^{-(L-1)} & a_k^{-(L-2)} & \cdots & 1 \end{bmatrix}$$

$$\mathbf{A} = \sum_{k=1}^{D} \mathbf{A}_k = \begin{bmatrix} D & \sum_{k=1}^{D} a_k & \cdots & \sum_{k=1}^{D} a_k^{L-1} \\ \sum_{k=1}^{D} a_k^{-1} & D & \cdots & \sum_{k=1}^{D} a_k^{L-2} \\ \vdots & \vdots & \ddots & \vdots \\ \sum_{k=1}^{D} a_k^{-(L-1)} & \cdots & \cdots & D \end{bmatrix}_{L \times L} \tag{A.1}$$

Clearly, if the rank of $\mathbf{A}$ is r, then there exists a submatrix within $\mathbf{A}$ of size $r \times r$ such that the determinant of the submatrix is nonzero [25]. Consider the submatrix $\mathbf{A}_D$ of size $D \times D$ of $\mathbf{A}$

$$\mathbf{A}_D = \begin{bmatrix} D & \sum_{k=1}^{D} a_k & \cdots & \sum_{k=1}^{D} a_k^{D-1} \\ \sum_{k=1}^{D} a_k^{-1} & D & \cdots & \sum_{k=1}^{D} a_k^{D-2} \\ \vdots & \vdots & \ddots & \vdots \\ \sum_{k=1}^{D} a_k^{-(D-1)} & \cdots & \cdots & D \end{bmatrix}_{D \times D}. \tag{A.2}$$

$\mathbf{A}_D$ can be decomposed into the multiplication of two $D \times D$ matrices given by $\mathbf{A}_D = \mathbf{B}_D \mathbf{C}_D$, where

$$\mathbf{B}_D = \begin{bmatrix} 1 & 1 & \cdots & 1 \\ a_1^{-1} & a_2^{-1} & \cdots & a_D^{-1} \\ a_1^{-2} & a_2^{-2} & \cdots & a_D^{-2} \\ \vdots & \vdots & \ddots & \vdots \\ a_1^{-(D-1)} & a_2^{-(D-1)} & \cdots & a_D^{-(D-1)} \end{bmatrix}_{D \times D}$$

$$\mathbf{C}_D = \begin{bmatrix} 1 & a_1 & \cdots & a_1^{(D-1)} \\ 1 & a_2 & \cdots & a_2^{(D-1)} \\ \vdots & \vdots & \ddots & \vdots \\ 1 & a_D & \cdots & a_D^{(D-1)} \end{bmatrix}_{D \times D}. \tag{A.3}$$

It is easy to see that $\mathbf{C}_D$ is a Vandermonde matrix of size D. The determinant of a Vandermonde matrix can be calculated by [25]

$$\det(\mathbf{C}_D) = \prod_{\substack{i,j \\ i>j}}^{D} (a_i - a_j) \tag{A.4}$$

which is nonzero, since $a_i \neq a_j$ for $i \neq j$, $1 \leq i, j \leq D \leq K$. Therefore, $\text{rank}(\mathbf{C}_D) = D$, and $\mathbf{C}_D$ is full rank. Since $a_k^{-1} = a_k^*$, $\mathbf{C}_D^H = \mathbf{B}_D$, and $\mathbf{B}_D$ is also full rank. This shows $\det(\mathbf{A}_D) = \det(\mathbf{B}_D)\det(\mathbf{C}_D)$ is nonzero, confirming $\mathbf{A}_D$ is a full-rank matrix with rank D. Since $\mathbf{A}_D$ is a submatrix of $\mathbf{A}$, then $\text{rank}(\mathbf{A}) \geq D = d_{\text{free}}$, concluding with $\text{rank}(\mathbf{A}) = D \leq L$.

If $L < D$, then $\mathbf{A}$ is a submatrix of $\mathbf{A}_D$. Again from (A.2), (A.3) and (A.4), $\mathbf{A}_D$ is a full-rank matrix with rank D, due to the fact that $a_i \neq a_j$ for $i \neq j$, $1 \leq i, j \leq D \leq K$. Since any submatrix of a full-rank matrix is also full rank, then the $L \times L$ matrix $\mathbf{A}$ is full rank with $\text{rank}(\mathbf{A}) = L$. Consequently, $\text{rank}(\mathbf{A}) = \min(D, L) = \min(d_{\text{free}}, L)$.

ACKNOWLEDGMENT

The authors would like to thank the anonymous reviewers, whose comments improved the development in the paper.

REFERENCES

[1] E. Zehavi, "8-PSK trellis codes for a Rayleigh channel," *IEEE Trans. Commun.*, vol. 40, no. 5, pp. 873–884, May 1992.

[2] G. Caire, G. Taricco, and E. Biglieri, "Bit-interleaved coded modulation," *IEEE Trans. Inf. Theory*, vol. 44, no. 3, pp. 927–946, May 1998.

[3] V. Tarokh, N. Seshadri, and A. Calderbank, "Space-time codes for high data rate wireless communication: Performance criterion and code construction," *IEEE Trans. Inf. Theory*, vol. 44, no. 2, pp. 744–765, Mar. 1998.

[4] S. M. Alamouti, "A simple transmit diversity technique for wireless communications," *IEEE J. Sel. Areas Commun.*, vol. 16, no. 8, pp. 1451–1458, Oct. 1998.

[5] V. Tarokh, H. Jafarkhani, and A. Calderbank, "Space-time block codes from orthogonal designs," *IEEE Trans. Inf. Theory*, vol. 45, no. 5, pp. 1456–1467, Jul. 1999.

[6] ——, "Space-time block coding for wireless communications: Performance results," *IEEE J. Sel. Areas Commun.*, vol. 17, no. 3, pp. 451–460, Mar. 1999.

[7] H. Bolcskei and A. J. Paulraj, "Space-frequency coded broadband OFDM systems," in *Proc. WCNC*, Sep. 2000, vol. 1, pp. 1–6.

[8] B. Lu and X. Wang, "Space-time code design in OFDM systems," in *Proc. IEEE GLOBECOM*, Nov. 27–Dec. 1, 2000, vol. 2, pp. 1000–1004.

[9] D. Agrawal, V. Tarokh, A. Naguib, and N. Seshadri, "Space-time coded OFDM for high data-rate wireless communication over wideband channels," in *Proc. VTC*, May 1998, vol. 3, pp. 2232–2236.

[10] H. Bolcskei and A. J. Paulraj, "Space-frequency codes for broadband fading systems," in *Proc. ISIT*, Jun. 2001, p. 219.

[11] H. El Gamal, A. R. Hammons, Jr., Y. Liu, M. P. Fitz, and O. Y. Takeshita, "On the design of space-time and space-frequency codes for MIMO frequency-selective fading channels," *IEEE Trans. Inf. Theory*, vol. 49, no. 9, pp. 2277–2292, Sep. 2003.

[12] Z. Liu and G. B. Giannakis, "Space-time-frequency coded OFDM over frequency-selective fading channels," *IEEE Trans. Signal Process.*, vol. 50, no. 10, pp. 2465–2476, Oct. 2002.

[13] I. Lee, A. M. Chan, and C. E. W. Sundberg, "Space-time bit interleaved coded modulation for OFDM systems in wireless LAN applications," in *Proc. IEEE ICC*, 2003, vol. 5, pp. 3413–3417.

[14] ——, "Space-time bit interleaved coded modulation for OFDM systems," *IEEE Trans. Signal Process.*, vol. 52, no. 3, pp. 820–825, Mar. 2004.

[15] Z. Hong and B. L. Hughes, "Robust space-time codes for broadband OFDM systems," in *Proc. IEEE WCNC*, Mar. 2002, vol. 4, pp. 105–108.

[16] D. Rende and T. F. Wong, "Bit-interleaved space-frequency coded modulation for OFDM systems," in *Proc. IEEE ICC*, May 2003, vol. 4, pp. 2827–2831.

[17] E. Akay and E. Ayanoglu, "Bit-interleaved coded modulation with space–time block codes for OFDM systems," in *Proc. IEEE VTC*, Los Angeles, CA, Sep. 2004, vol. 4, pp. 2477–2481.

[18] ——, "Full frequency diversity codes for single input single output systems," in *Proc. IEEE VTC*, Los Angeles, CA, Sep. 2004, vol. 3, pp. 1870–1874.

[19] H. Jafarkhani and N. Seshadri, "Super-orthogonal space-time trellis codes," *IEEE Trans. Inf. Theory*, vol. 49, no. 4, pp. 937–950, Apr. 2003.

[20] *Wireless LAN Medium Access Control (MAC) and Physical Layer (PHY) Specifications. High-Speed Physical Layer in the 5 GHz Band*, IEEE 802.11a, IEEE [Online]. Available: http://standards.ieee.org/getieee802/802.11.html

[21] U. Wachsmann, R. F. H. Fischer, and J. B. Huber, "Multilevel codes: Theoretical concepts and practical design rules," *IEEE Trans. Inf. Theory*, vol. 45, no. 5, pp. 1361–1391, Jul. 1999.

[22] X. Li and J. A. Ritcey, *Trellis-Coded Modulation With Bit Interleaving and Iterative Decoding*, vol. 17, no. 4, pp. 715–724, Apr. 1999.

[23] S. Lin and D. J. Costello, *Error Control Coding: Fundamentals and Applications*. Englewood Cliffs, NJ: Prentice-Hall, 1983.

[24] Y. Liu, M. P. Fitz, and O. Y. Takeshita, "Outage probability and space-time code design criteria for frequency selective fading channels with fractional delay," in *Proc. IEEE ISIT*, Jun. 2001, p. 80.

[25] R. A. Horn and C. R. Johnson, *Matrix Analysis*. Cambridge, U.K.: Cambridge Univ. Press, 1990.

[26] E. Akay and E. Ayanoglu, "Low complexity decoding of bit-interleaved coded modulation," in *Proc. IEEE ICC*, Paris, France, Jun. 2004, vol. 2, pp. 901–905.

[27] ——, "High performance Viterbi decoder for OFDM systems," in *Proc. IEEE VTC*, Milan, Italy, May 2004, vol. 1, pp. 323–327.

[28] H. Jafarkhani, *Space-Time Coding: Theory and Practice*. Cambridge, U.K.: Cambridge Univ. Press, 2005.

[29] E. Akay and E. Ayanoglu, "Low complexity decoding of BICM STBC," in *Proc. IEEE VTC* , Stockholm, Sweden, May 2005, vol. 2, pp. 715–718.

[30] *TGn Channel Models*, IEEE 802.11-03/940r2, IEEE [Online]. Available: ftp://ieee:wireless@ftp.802wirelessworld.com/11/03/11-03-0940-02-000n-tgn-channel-models.doc

[31] *Intelligent Multi-Element Transmit and Receive Antennas I-METRA*, IST-2000-30148, IST [Online]. Available: http://www.ist-imetra.org/

[32] J. P. Kermoal, L. Schumacher, K. I. Pedersen, P. E. Mogensen, and F. Frederiksen, "A stochastic MIMO radio channel model with experimental validation," *IEEE J. Sel. Areas Commun.*, vol. 20, no. 6, pp. 1211–1226, Aug. 2002.

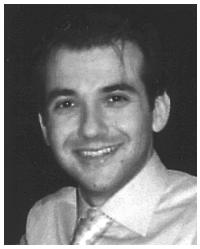

Enis Akay (S'98) received the B.S. degree in electrical and electronics engineering from Middle East Technical University, Ankara, Turkey, in 1995, and the M.S. and Ph.D. degrees in electrical and computer engineering from the University of California, Irvine in 2001 and 2006, respectively.

From 2003 to 2006, he was with the Center for Pervasive Communications and Computing where he was a Graduate Student Researcher. His research interests are wireless MIMO systems, wireless LANs, beamforming, space–time coding, MIMO-OFDM, BICM, coding, and coded modulation.

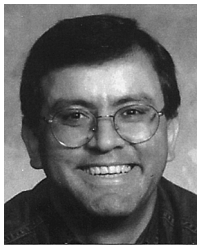

Ender Ayanoglu (S'82–M'85–SM'90–F'98) received the B.S. degree from the Middle East Technical University, Ankara, Turkey, in 1980, and the M.S. and Ph.D. degrees from Stanford University, Stanford, CA, in 1982 and 1986, respectively, all in electrical engineering.

He was with the Communications Systems Research Laboratory of AT&T Bell Laboratories (Bell Labs, Lucent Technologies after 1996) until 1999, and was with Cisco Systems until 2002. Since 2002, he has been with the Department of Electrical Engineering and Computer Science, Henry Samueli School of Engineering, University of California, Irvine, where he is a Professor. He serves as Director of the Center for Pervasive Communications and Computing and holds the Conexant-Broadcom Endowed Chair at UC Irvine.

Since 1993, he served as an Editor of the IEEE TRANSACTIONS ON COMMUNICATIONS, and currently serves as its Editor-in-Chief. He was on the cabinet of the IEEE Communications Society Communication Theory Committee from 1990 until 2002, and served as its chair 1999–2001. He was the recipient of the IEEE Communications Society Stephen O. Rice Prize Paper Award in 1995, and the IEEE Communications Society Best Tutorial Paper Award in 1997.